Adsorption of small hydrocarbon radicals on single walled carbon nanotubes of finite length

Jianhua Wu
Department of Physics, Atmospheric Sciences, and Geoscience, Jackson State University, Jackson, Mississippi 39217, USA

Frank Hagelberg
Department of Physics and Astronomy, East Tennessee State University, Johnson City, Tennessee 37614, USA

(Received 23 October 2009; revised manuscript received 18 January 2010; published 2 April 2010)

Adsorption of the hydrocarbon radicals CH, CH_2, and CH_3 on finite single walled carbon nanotubes (SWNTs) of the (10,0) type is investigated by density-functional theory (DFT). Two classes of finite SWNTs are considered: truncated SWNTs, where admission is made for geometric reconstruction of the tube ends, and those capped with fullerene hemispheres. Both prototypes are characterized by ground states with nonvanishing magnetic moments, where antiferromagnetic coordination between nds is preferred over the ferromagnetic alternative. The focus of this study is on the influence exerted by the adsorbates on the magnetic structure of the system as a whole, as well as the relative impact of both, confinement due to the finite lengths of the considered SWNTs and their magnetic structure on the preferred positions of hydrocarbon adsorbates. In particular, it is shown that the confinement outweighs the magnetic effect in defining the adsorption energy variations among nonequivalent sites of attachment. The SWNT spin-density distributions turn out to affect the nature of the bonding between finite SWNT substrates and hydrocarbon radical adsorbates.

DOI: 10.1103/PhysRevB.81.155407 PACS number(s): 61.48.De, 68.43.Mn, 75.50.Xx, 87.14.Df

I. INTRODUCTION

Reactions between single walled carbon nanotubes (SWNTs) and exohedral adsorbates are studied for both their systematic interest and their technological relevance. A variety of applications has been identified for SWNTs functionalized with external species. Thus, combining them with Ca adsorbates may yield devices for high capacity hydrogen storage, as was pointed out recently.[1] Environmental applications of SWNTs capitalize on the changes induced in the materials properties of the SWNT by the presence of an externally adsorbed species. For instance, the well-known impact exerted by adsorbed gas molecules on the conductivity of semiconducting SWNTs has been exploited to design nanotube molecular sensors which react faster and with substantially higher sensitivity than existing solid-state sensors.[2] Understanding the elementary processes that underlie this technology requires detailed knowledge of the interaction between organic species and the SWNT surface.

SWNTs with externally attached hydrocarbon radicals have been the subject of several recent studies, from the sides of both experiment[3] and theory.[4–7] The interest in the interaction between SWNTs and hydrocarbon radicals is rooted in its relevance to the catalyst assisted chemical vapor deposition (CVD) method which allows for the controlled growth of SWNTs with few structural defects.[4,5] Using this technique, one fabricates SWNTs from a hydrocarbon precursor gas.[5,8] The primary hydrocarbon gas molecules, e.g., C_2H_2 or CH_4, react dissociatively with transition metal catalysts. The resulting hydrocarbon radicals contribute to SWNT synthesis by providing C atoms that are readily incorporated into the growing SWNT. The presence of small hydrocarbon species, namely CH_2 and CH_3, as exohedral adsorbates on the SWNT surface has been established by Fourier transform infrared (FTIR) spectroscopy.[3] Employing a tight-binding approach, Zhou[4] and He[6] considered the adsorption of CH, CH_2, and CH_3 on a zigzag SWNT of the (9,0) type and modeled the interaction of these species with various structural SWNT defects. In conclusion, they ascribed an annealing effect to the hydrocarbon adsorbates, as a consequence of their preferential interaction with dangling bonds of the SWNT substrate. The interaction between the regular, defect-free SWNT surface, and external hydrocarbon radicals is distinctly weaker.

The theoretical work devoted so far to hydrocarbon molecules attaching to SWNTs made reference to periodic SWNTs. Finite, i.e., axially bounded SWNTs, however, attract much current attention.[9–13] This interest is largely motivated by the prospect of developing these units into nanotechnological devices as diverse as nanopharmaceuticals[14] and transmission elements in molecular electronics.[12,13] On a more fundamental level, it has been noted that finite SWNTs of the zigzag type are intrinsically magnetic for a dimensional reason: magnetism emerges here as the periodic system is reduced to finite length. Unpaired electrons localizing at the edges of the finite structure impose magnetic boundary condition on the system as a whole, and so exert a spin polarizing effect on the delocalized π electrons in the interior of the SWNT.

In a recent density-functional theory (DFT) treatment of (10,0) SWNTs at varying lengths,[11] this phenomenon was studied as a function of the tube termination mode. Three prototypes were considered, differing from each other with respect to the tube—terminating structures. Specifically, (a) SWNTs with hydrogen termination, (b) truncated SWNTs where admission is made for geometric reconstruction of the tube ends and those (c) those capped with fullerene hemispheres were included in this comparison.

The ground states of the investigated structures turned out to favor antiferromagnetic (AFM) coordination, associated with opposite spin orientations at the two edges of the tube. Metastable ferromagnetic (FM) and also, well separated from the magnetic solutions, nonmagnetic states were obtained as well. The observed preference of AFM ordering is in accor-

dance with an expectation based on Lieb's theorem[15] related to the ground-state spin of bipartite lattices. From this statement, the total spin of a bipartite lattice composed of two equal interpenetrating sublattices at half-filling, such as graphene, is zero. While the proof of Lieb's theorem operates with the Hubbard Hamiltonian,[16] it's contents have exhibited a certain robustness with respect to the quantum mechanical approach applied and also been confirmed by DFT computation (see, e.g., Refs. 17 and 18). AFM order was established for *zigzag graphene nanoribbons (*ZGNRs) which are graphene sheets reduced to finite size in both dimensions. These in turn may be understood as finite zigzag SWNTs unrolled into a plane. Since the latter operation does not affect the edge structure of the two systems, the persistence of AFM order in finite zigzag SWNTs is not surprising. We add that degeneracy of the two magnetic phases was found for capped SWNTs (c) beyond a critical length. Being fullerene—nanotube hybrids, these deviate more strongly than the structural types (a) and (b) from the bipartite lattice model realized by graphene such that the predominance of AFM coordination is anticipated to a lesser extent for capped than for truncated or hydrogenated systems.

A technologically interesting feature shared by both, ZGNRs and finite SWNTs is *half-metallicity*.[12,13,18,19] Due to the strong localization of electrons with opposite spin orientations at the ends of the SWNT, an axially applied electric field may cause the disappearance of the highest occupied molecular orbital-lowest unoccupied molecular orbital energy difference selectively for one spin channel while keeping the gap at a finite value for the other.[12,13] Electric conductivity is then confined to electrons of a well-defined spin orientation, a condition of basic relevance for applications in the emerging field of spintronics.

Combining the available information on hydrocarbons attaching to periodic SWNTs with that on finite SWNT magnetism, we address in this contribution three main problems: what is the relative impact of the confinement due to the finite lengths of the considered SWNT substrates and the magnetic structure of the SWNT on the geometric and energetic features of hydrocarbon radical adsorption? How do small hydrocarbon adsorbates affect the electronic, magnetic and energetic properties of a zigzag SWNT? To what extent do the answers to these two questions change with the particular choice of hydrocarbon adsorbate? In continuation of our earlier work, we will treat these issues by considering the interaction of a finite (10,0) SWNT with the species CH, CH_2, and CH_3.

II. COMPUTATIONAL DETAILS

DFT[20] calculations have been performed using the Vienna *ab initio* simulation package code.[21,22] The finite-temperature version of local density functional theory, as developed by Mermin,[23] was employed in conjunction with the exchange-correlation functional given by Ceperley and Alder and parameterized by Perdew and Zunger.[24] Instead of Fermi-Dirac broadening of the one-electron energy levels, Gaussian broadening was used. The width of the Gaussian distribution was selected as 0.01eV, the total energy of the system referring to the limit of vanishing width.

The generalized Kohn-Sham equations were solved utilizing a residual minimization scheme, namely the direct inversion in the iterative subspace (RMM-DIIS) method.[25,26] The interaction of valence electrons and core ions was described by the projector-augmented wave method.[27] The Perdew-Burke-Ernzerhof[28]generalized gradient correction for the exchange-correlation functional was used in all computations.

Periodic boundary conditions were imposed on a unit cell of dimension $20\times20\times40$ Å^3 for the adsorption of hydrocarbon radicals on a finite-size SWNTs. The tube axis was oriented along the z direction. We included only the Γ point of the Brillouin zone. For the adsorption studies involving a periodic SWNT, a $20\times20\times21.37$ Å^3 unit cell was used. Here the unit cell contained 200 carbon atoms, corresponding to a length L=10. Finally, the geometry was optimized, enforcing a total energy difference between two subsequent steps of less than 1 meV as convergence criterion.

The adsorption energy is defined as

$$E_{ads} = E_{SWNT} + E_{CHn} - E_{SWNT+CHn},$$

where E_{SWNT} stands for the energy of the pure SWNT, E_{CHn}, with n=1–3, for the energy of a hydrocarbon radical, and $E_{SWNT+CHn}$ for the energy of the combined system.

In some selected cases, we assessed our DFT results, involving a plane wave basis, by comparison with quantum chemical calculations, using a Gaussian basis. Employing the latter approach, we performed additional geometry optimizations on reduced models of the pure SWNTs considered in this work, namely, truncated and capped SWNTs containing 120 C atoms, by use of the B3LYP potential in conjunction with the 6–31 G basis set.[29] The difference between the C-C bond lengths obtained by the two alternative methods is limited by 1 per cent in all cases considered. Further, both alternative approaches yielded the same ground state multiplicities.

III. RESULTS AND DISCUSSION

In this section, we define the systems under study, followed by a description of their geometric and energetic features as obtained from our DFT calculations and a discussion of their electronic and magnetic properties. In continuation of our earlier work on finite SWNTs,[11] we adopt a (10,0) system with 240 carbon atoms. This corresponds to a length L=11 for a truncated SWNT and L=10 for capped SWNT, where we define L as the number of transpolyene chains contained in the SWNT. Figure 1 shows the two prototypes included. They differ from each other with respect to the termination mode. Specifically, we included truncated SWNTS where allowance is made for geometric reconstruction of the cylinder ends [Figs. 1(a) and 1(c)], and SWNTs capped at both ends by addition of C_{60} hemispheres [Figs. 1(b) and 1(d)].

A. Geometric and energetic properties

Finite SWNTs pose a more demanding adsorption problem than their periodic counterparts. If an ideal (defect-free)

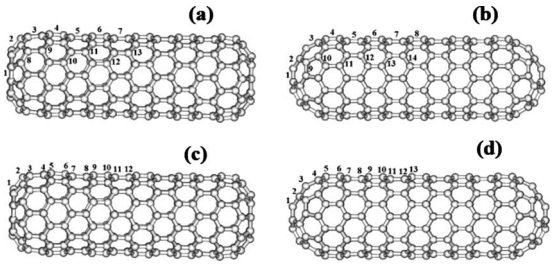

FIG. 1. Initial adsorption sites for CH and CH_2 in contact with the truncated (a) and the capped (b) SWNT, and CH_3 in contact with truncated (c) and the capped (d) SWNT.

infinite SWNT is considered, five basic cases of adsorption can be distinguished, corresponding to the attachment of the external species to a hollow site, i.e., a hexagon center, as well as to the two nonequivalent C sites and C-C bonds present in the SWNT which we will refer to as particle and bridge sites, respectively. In an initial step, we examined adsorption to particle, bridge, and hollow sites of an ideal periodic (10,0) system for the three radicals included, CH, CH_2, and CH_3. The hollow site was found to be substantially less stable than the alternative stable configurations, being about 2.0 eV higher than these in adsorption energy. For both CH and CH_2, particle sites were seen to be unstable, as both species were found to migrate to bridge sites when initially attached to particle locations. In the case of CH_3, three carbon bonds are saturated by hydrogen atoms, and therefore, interaction takes place chiefly with a single SWNT atom. Consequently, CH_3 attaches preferentially to a particle site. These findings agree with the observations communicated in.[4,6]

Turning to finite SWNTs, a considerably larger number of nonequivalent sites are identified than for the ideal periodic system. We approached the question for the preferred adsorption geometries by defining characteristic locations on the nanotube surface, extending from nd to the central section of the tube. The initial adsorbate positions for CH and CH_2, comprising all nonequivalent axial and tangential C-C bonds are indicated in Figs. 1(a) and 1(b) for the cases of a truncated and a capped SWNT substrate, respectively. The corresponding scheme for CH_3 adsorption is shown in Figs. 1(c) and 1(d), involving particle positions as initial places of attachment.

Typical adsorption geometries on capped SWNTs are shown in Fig. 2 for (a) CH and (b) CH_2. From these arrangements, the C constituent of CH realizes sp^2 bonding while that of CH_2, coordinating a C-C and an H-H group at right angle to each other, exhibits sp^3 bonding. However, symmetric attachment, involving two C-C bonds of equal distance

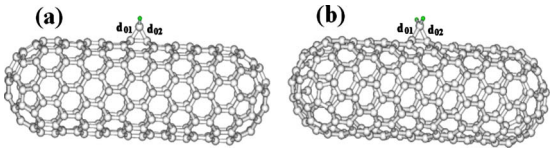

FIG. 2. (Color online) Adsorption geometries of CH (a) and CH_2 (b) at center sites of the capped (10,0) SWNT.

between the substrate and the adsorbate, is only found for symmetric axial bridge sites. These are, with reference to Figs. 1(a) and 1(b), the sites 1 and 7 (1 and 8) for truncated (capped) SWNTs. In both cases, the C-C bond is parallel to the tube axis and connects SWNT atoms in equivalent positions. The maximum bond length deviations are about three per cent for the case of a truncated SWNT. CH and CH_2 interaction with ideal periodic SWNTs leads to more regular bonding patterns.[4–7] Here, axial SWNT bonds give rise to symmetric and tangential to asymmetric attachment.

For both SWNT substrate types, the adsorption bond lengths of CH are systematically shorter than those of CH_2 (for quantitative confirmation of this effect in case of truncated SWNT substrates, see the Table included as supplementary material,[30] containing C-C bond lengths for CH and CH_2 adsorbates), documenting a somewhat stronger substrate-adsorbate interaction in the former than in the latter case which in turn reflects the higher degree of under coordination of CH in comparison with CH_2. This feature is also manifested by the relation between the adsorption energies of CH and CH_2 listed in Table I, the former exceeding the latter at any given site.

The observed increase of the C-C bond lengths from the end to the center of the truncated SWNT for axial adsorption of CH and CH_2 is a reflection of the corresponding decrease in interaction strength. The adsorption energy values listed in Table I as a function of the attachment site are in accordance with this trend, reducing dramatically from site 1 to site 5 where they attain a near-constant value of 2.62 eV (2.58 eV) for CH (CH_2). The drop in adsorption energy is related to the gradual reduction in bond strain as one goes from nd to the center. Thus, the next neighbor distance within the terminating decagon of the pure truncated L=11 SWNT (1.451 Å) diminishes to a value of 1.423 Å for the axial bond length in the midsection of the tube. This is close to the axial bond length of the periodic system, 1.422 Å. The maximally strained C-C bond of the substrate is associated with the maximum adsorption energy for CH (CH_2). We also note that at places of strong interaction between the substrate and the adsorbate, as documented by high adsorption energy values, the energy gap of the composite system is markedly lower than that of the pure SWNT. The energy gap, however, converges toward the pure SWNT value as CH (CH_2) approaches the tube center site.

Inspecting CH (CH_2) adsorption on the periodic (10,0) SWNT, we find adsorption energy values of 2.623 eV (2.595 eV) for the axial and 3.343 eV (3.067 eV) for the tangential sites of attachment. This is to be compared with the respective adsorption energies for the periodic (9,0) SWNT, as reported in Refs. 4 and 6 where an equally pronounced preference for tangential as compared with axial sites was found, ranging also in the order of 0.5 eV. This preference is in keeping with the observation that the tangential bonds tend to be longer by about 0.5% than the axial bonds, manifesting stronger interaction between adjacent C atoms of the SWNT for the latter. In the context of CH (CH_2) adsorption on finite truncated SWNTs, we note, with reference to Table I that the adsorption energies for both bond types tend toward the periodic case in the midsection of the tube.

We now focus on the capped SWNT in combination with CH and CH_2. The capped species contains two junctions be-

TABLE I. Quantities relevant for the energetic and magnetic properties of (a) CH, (b) CH_2, and (c) CH_3 adsorption on truncated and capped (10,0) SWNTs. All energies are indicated in eV, magnetic moments in μ_B.

(a)

	CH on truncated SWNT				CH on capped SWNT			
Position	E_{ads} [a]	$E_{FM}-E_{AFM}$ [b]	E_{gap} [c]	m_{FM} [d]	E_{adsorp}	$E_{FM}-E_{AFM}$	E_{gap}	m_{FM}
1	7.985	0.004	0.345	5	4.274	0.000	0.114	1
2	5.343	0.005	0.368	5	4.502	0.000	0.092	1
3	4.464	0.003	0.337	7	5.141	0.000	0.049	1
4	2.631	0.008	0.396	7	3.837	0.000	0.082	1
5	2.592	0.008	0.441	7	2.915	0.001	0.090	3
6	2.611	0.008	0.472	7	2.706	0.001	0.089	3
7	2.608	0.008	0.486	5	2.833	0.002	0.120	1
8	3.765	0.005	0.232	7	2.722	0.000	0.113	1
9	4.139	0.006	0.361	7	4.314	0.000	0.043	1
10	3.372	0.006	0.392	7	4.277	0.000	0.046	1
11	3.291	0.006	0.457	7	3.840	0.000	0.048	1
12	3.344	0.009	0.479	7	3.441	0.000	0.100	1
13	3.351	0.007	0.482	7	3.352	0.000	0.112	1
14					3.402	0.000	0.120	1
Pure SWNT		0.008	0.482	6	N/A	0.006	0.119	2

(b)

	CH_2 on truncated SWNT				CH_2 on capped SWNT			
Position	E_{adsorp}	$E_{FM}-E_{AFM}$	E_{gap}	m_{FM}	E_{adsorp}	$E_{FM}-E_{AFM}$	E_{gap}	m_{FM}
1	5.131	0.006	0.146	6	3.997	0.000	0.073	0
2	4.557	0.007	0.374	6	3.739	0.001	0.082	2
3	3.751	0.007	0.383	6	3.923	0.000	0.044	0
4	2.606	0.007	0.463	6	2.953	0.001	0.065	2
5	2.564	0.008	0.468	6	2.886	0.001	0.084	2
6	2.578	0.008	0.476	6	2.680	0.002	0.092	2
7	2.580	0.009	0.486	6	2.808	0.002	0.109	2
8	3.696	0.005	0.217	6	2.698	0.002	0.113	2
9	3.851	0.007	0.444	6	3.565	0.000	0.041	0
10	3.098	0.007	0.421	6	3.569	0.000	0.092	0
11	3.028	0.007	0.476	6	3.374	0.002	0.101	2
12	3.071	0.007	0.481	6	3.144	0.002	0.110	2
13	3.072	0.007	0.485	6	3.059	0.002	0.112	2
14					3.114	0.002	0.116	2
Pure SWNT		0.008	0.482	6	N/A	0.006	0.119	2

(c)

	CH_3 on truncated SWNT					CH_3 on capped SWNT				
Position	E_{adsorp}	$E_{FM}-E_{AFM}$	E_{gap}	m_{FM}	$E_{NM}-E_{AFM}$	E_{adsorp}	$E_{FM}-E_{AFM}$	E_{gap}	m_{FM}	$E_{NM}-E_{AFM}$
1	2.009	0.005	0.370	5	0.670	2.422	0.000	0.115	1	0.040
2	2.708	0.005	0.370	5	0.660	1.374	0.000	0.032	1	0.027
3	1.431	0.005	0.166	5	0.689	2.298	0.000	0.065	1	0.036
4	1.810	0.005	0.432	5	0.677	2.272	0.001	0.079	1	0.037
5	0.886	0.006	0.220	7	0.751	1.325	0.001	0.107	1	0.041
6	1.135	0.007	0.435	5	0.675	1.330	0.001	0.018	1	0.035
7	0.818	0.008	0.221	7	0.809	1.271	0.001	0.013	1	0.022
8	0.897	0.014	0.312	5	0.684	1.204	0.001	0.072	1	0.041
9	0.816	0.011	0.246	7	0.829	0.999	0.001	0.039	1	0.036
10	0.840	0.057	0.238	7	0.754	0.955	0.001	0.085	1	0.040
11	0.771	0.015	0.233	7	0.830	0.880	0.000	0.026	1	0.033
12	0.800	0.025	0.227	7	0.805	1.004	0.000	0.079	1	0.037
13						1.073	0.000	0.042	1	0.035
Pure SWNT		0.008	0.482	6	0.877		0.006	0.119	2	0.080

[a]Adsorption energy.
[b]Energy difference between the ground-state energies for the ferromagnetic and the antiferromagnetic case.
[c]Energy gap.
[d]Magnetic moment for ferromagnetic coordination.

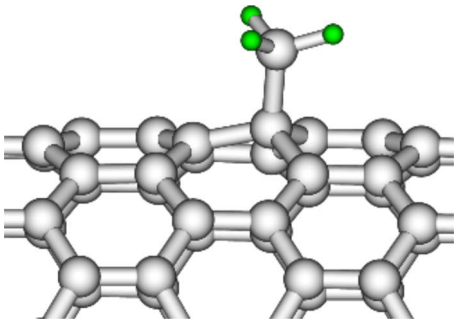

FIG. 3. (Color online) Local deformation due to CH_3 adsorbed at a center site of the truncated (10,0) SWNT.

tween two different carbon nanostructures. The matching between the SWNT and the C_{60} hemisphere edges impose strain on the system as a whole. This strain manifests itself in the equilibrium geometry of the pure capped SWNT by a staggering behavior of the bonds that connect the two subsystems [see site 4 in Fig. 1(b) for the location of the matching zone]. More specifically, the bonds that link a cap pentagon and an SWNT hexagon are approximately 1.40 Å in length, while those between two hexagons average to 1.44 Å. For the axial bridge positions of both CH and CH_2 [1–8 in Fig. 1(b)], a maximum of the adsorption energy is found at site 3, and thus in close proximity to the matching zone between the caps and the SWNT. Analogous observations are made for the tangential bridge positions [9–14 in Fig. 1(b)]. For both types of bonds, the adsorption energy decreases steadily toward the tube center. In parallel with the case of a truncated SWNT substrate, as discussed above, the energy gap of the capped species evolves toward the pure SWNT limit as the adsorbates move from the maximally strained region to the tube center. With respect to the comparison between the adsorption energies of the finite and the infinite SWNT substrate, analogous observations are made for the capped as for the truncated case.

The bond lengths for attachment at axial sites increase monotonically from the end to the center of the SWNT. This trend is not only observed for CH and CH_2, but also for CH_3 adsorption where the C-CH_3 distance elongates by 1.3% (2.3%) as one goes from the end to the center of the truncated (capped) SWNT. As demonstrated by Fig. 3, CH_3 attachment causes local substrate deformation as the SWNT atom is lifted toward the adsorbate. CH_3 adsorption thus induces strain into the next-neighbor bonds of the attacked SWNT atom, corresponding to a certain amount of pyramidalization and thus departure from sp^2 coordination. While this phenomenon is also observed for periodic SWNTs,[7] the electronic structure and the pattern of the adsorption energies of finite zigzag SWNTs in contact with a hydrocarbon radical differ substantially from those of their periodic counterparts. These deviations are rooted in both the confinement effect and the magnetism characteristic of the former system, as will be discussed in the following subsection.

B. Electronic and magnetic properties

Figure 4 shows a comparison between the linear spin density profiles of the two SWNT substrates considered here, (a)

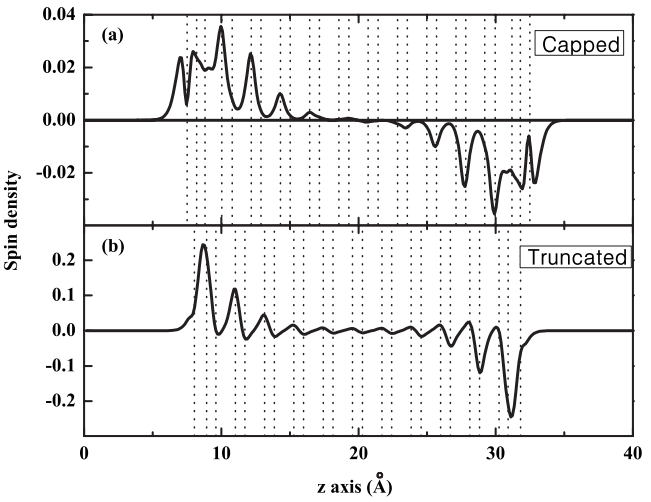

FIG. 4. Representations of the linear spin density (in 1/Å) for the capped L=10 (a) and the truncated L=11 (b) SWNT versus the tube length coordinate. The perpendicular dotted lines are the locations of the atomic layers.

truncated and (b) terminated by C_{60} hemispheres. Both systems are represented in AFM coordination which, from our computations, was found to be the magnetic phase of highest stability. In both cases, localization of unpaired electrons gives rise to the observed spin distribution. The reason for the appearance of under coordination, however, is different for the two systems. SWNT truncation leads to dangling bonds which localize at dges, capping results in partially strained and partially broken bonds between the fullerene and the tube segment of the unit, causing finite spin density to emerge in the matching region between the two system components. The nonvanishing spin density located in the cap region is correlated with the occurrence of a considerable variation in the C-C bond lengths between atoms present in the caps. Thus, the different bond lengths found in the cap terminating pentagon are 1.450, 1.434, and 1.423 Å, and thus deviate from each other by up to 2 per cent, while a single bond length (1.450 Å) is found for the distance between adjacent C atoms in the terminating pentagon of C_{60}. Capping the finite tube with fullerene halves yields a partial release of the edge strain present in the truncated system, as manifested by the difference between the local magnetic moments in the two cases, amounting to 3 μ_B for the truncated and 1 μ_B for the capped species.

How does this assessment change when hydrocarbon radicals attach to either SWNT type? While the essential features of the spin distributions shown in Figs. 4(a) and 4(b) are maintained, we note some characteristic variations as admission is made for hydrocarbon adsorption. As a general observation that pertains to both CH and CH_2, the presence of the adsorbing species does not change the preference of AFM order for the system as whole, as can be seen from the difference between the ground-state energies E_{FM} and E_{AFM} included in Table I.

Focusing on CH, we now inspect the truncated system in more detail. The spin density distributions for selected sites of CH attaching to the truncated substrate are shown in Fig. 5(a). Specifically, we include the sites 1, 2, 3, and 7, with

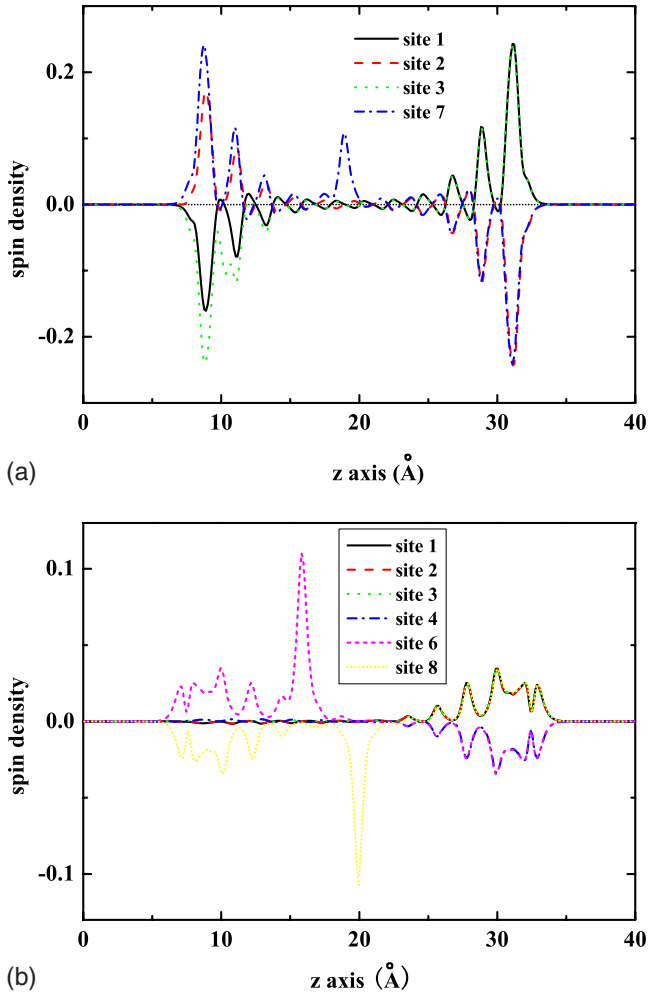

FIG. 5. (Color online) Representations of the linear spin density (in 1/Å) for the truncated L=11 SWNT (a) and the capped L=10 (b) with CH adsorbed at selected sites, versus the tube length coordinate.

reference to Fig. 1(a). The first two sites are in the region of dge, where the spin density is maximum [see Fig. 4(b)]. Here the local magnetic moment is reduced from 3 to 2 μ_B, indicating a covalent connection formed between two unpaired electrons, contributed by CH and by the SWNT edge. Accordingly, the spin density associated with these two sites shows a markedly diminished maximum on the SWNT side of CH attachment. However, the localization of the SWNT dangling bonds at dges implies a shift in the bonding pattern as one goes toward the SWNT center. For sites 3 to 7, the overall spin-density distribution can be described as a superposition between that of the pure SWNT and that of the CH adsorbate. This interpretation is supported by the rise of the energy difference between the AFM and the FM phase as one goes from site 1 to site 7, saturating at 8 meV, the value found for the pure truncated SWNT. Also, the diminishing tendency of the adsorption energy from dge to the center, which was mentioned above in the context of geometry, reflects the decrease in the mutual influence of the two subsystems on each other. At sites 3 to 6, the CH spin aligns with the spin of the SWNT edge closest to it. Site 7, being closest to the tube center, seems to represent an exception to this rule, as a state with $m_{FM}=5$ μ_B is found maximally stable in this case. The competing state with $m_{FM}=7$ μ_B, however, is seen to be higher in energy only by 2 meV. Therefore, within the accuracy of the procedure used in this work, it may be concluded that both magnetic states are degenerate in the midsection of the tube.

Turning to CH adsorbed on the capped SWNT, we find a similar pattern realized, with some significant changes. First, for the capped substrate, the two competing magnetic phases become degenerate upon adsorption. Second, while adsorption at or close to the tube center once more results in the pure SWNT spin-density distribution with an admixture due to the molecule [sites 6 and 8 in Fig. 5(b)], the interaction of CH with the tube close to its edges is more complex here than for the truncated substrate. In more detail, we identify a configuration which is typical for CH attachment to the matching regime between the fullerene hemisphere and the nanotube subsystem. Among the cases selected for inclusion in Fig. 5(b), this configuration is represented by sites 1–4. The spin density on the adsorbate side of the SWNT vanishes as a consequence of covalent bonding between two unpaired electrons localized at the CH molecule and in the matching zone. The mechanism is the same as that specified above for edge adsorption at sites 1 and 2 of the truncated tube [see Fig. 5(a)] where it results in a reduction of the spin density as opposed to its annihilation as observed here. For CH adsorbed at sites 1–4, the magnetic moment of the structure as a whole is localized in the matching zone farthest from the adsorbate.

The sites not shown in Fig. 5(b) (5, 7, 9–14) follow the models set by sites 1–4 (site 9–11) and 6–8 (sites 5, 7, 12–14).

Lastly, we comment on our results on CH_3 in contact with both SWNT types included here, as summarized in Table Ic. The most pronounced changes from CH and CH_2 to CH_3 adsorption are related to the preference of bridge sites in the former and particle sites in the latter case. From site 1 to site 9, we observe a marked even—odd staggering in the adsorption energy, and a similar behavior of the energy gap. No adsorption energy change is found for periodic SWNTs between the A (even labels according to the notation used here) and B (odd labels) sites of the generating graphene lattice.[6] This degeneracy with respect to the adsorption energy is removed as the SWNT is reduced to finite length. This effect is in accordance with the linear spin-density profile displayed in Fig. 4(b): the even-numbered sites coincide with places of maximum unpaired electron density, the odd-numbered, in contrast, with minima. Therefore, covalent bonds will be generated preferentially at the former sites. At the odd-numbered sites with $n>3$, as well as at general sites with $n>9$, where n is the site index, the local spin density is almost vanishing. CH_3 adsorption proceeds here according to the pattern described for periodic substrates:[4–7] to form a covalent bond between the SWNT and the molecule, an SWNT π bond is broken and traded for a sigma bond that connects the two subsystems. In these cases, adsorption gives rise to an additional spin, and the overall magnetic moment of the species is 7 μ_B, while 5 μ_B is favored at places of substantial spin density. This trend is clearly reflected by the CH_3 adsorption energies listed in Table I: at all

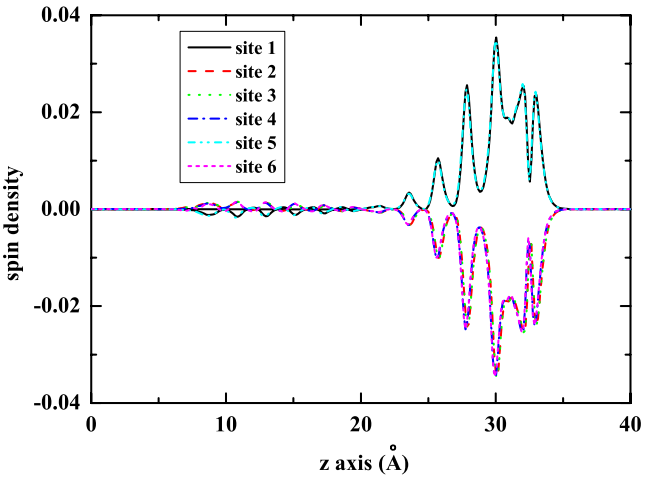

FIG. 6. (Color online) Representation of the linear spin density (in 1/Å) for the capped L=10 SWNT with CH_3 adsorbed at selected sites, versus the tube length coordinate.

sites with $m_{FM}=7\ \mu_B$, E_{ads} is substantially closer to the value found for the periodic (10,0) substrate, which we determine to be 0.814 eV, than at the sites with $m_{FM}=5\ \mu_B$.

For explaining the quantitative variation in the adsorption energy as a function of adsorbate position, however, the confinement effect due to SWNT reduction to finite length dominates the impact of SWNT magnetism by a substantial margin. This follows from additional calculations on artificial nonmagnetic systems ($m_{FM}=0$), involving CH_3 adsorbed on the truncated and capped SWNT substrates. The difference between the total energies for the nonmagnetic and the antiferromagnetic case, as included in Table I exhibits, for a given spin multiplicity, only slight changes in the order of 10 meV while the adsorption energy differences are in the eV range. From the data recorded for the truncated substrate in Table I, however, the magnetic state of the system exerts some influence on the energy difference between the nonmagnetic and the antiferromagnetic phase. Taking the nonmagnetic unit as a reference, the antiferromagnetic species with the higher spin multiplicity (corresponding to $m_{FM}=7$) are found to be more stable by an energy difference of about 0.15 eV than those with the lower multiplicity ($m_{FM}=5$). In the former case, the substrate spin configuration is the same as for the pure truncated SWNT. In addition, for selected positions of CH_3 on the truncated substrate, solutions with m=1 were identified. These were found to differ from the antiferromagnetic ground states by energy margins varying from 0.2 eV to a few meV while displaying a similar trend of the adsorption energy as a function of the attachment site.

The linear spin-density distributions characteristic of the CH_3 interaction with the capped SWNT, as shown in Fig. 6, present a uniform picture: bonding of the adsorbate to the SWNT annihilates the local magnetic moment of nd where the molecule locates, which is indicative of covalent bonding between the two subsystems.

From our analysis, the stability pattern of small hydrocarbon radicals on a truncated or capped semiconducting zigzag nanotube is substantially impacted by the confinement effect while the observed bonding features are accounted for by the distribution of the unpaired electron density along the tube surface and thus reflect finite SWNT magnetism.

IV. SUMMARY AND CONCLUSION

Adsorption of hydrocarbon radicals on finite SWNTs differs substantially from the previously considered adsorption on periodic SWNT. The former system is characterized by a much higher number of nonequivalent adsorption sites than the latter, corresponding to a large multiplicity of different adsorbate positions. Less obviously, finite SWNTs deviate from their periodic counterparts due to their nonvanishing magnetic moments which are attributed to the strain induced in the system due to tube termination. In this study, two termination modes are explored, namely, tube truncation preceding geometric relaxation of nds and addition of fullerene hemispheres to the edges of the truncated SWNTs.

From DFT computation, bridge positions are preferred by CH and CH_2, while CH_3 favors attachment to on-top sites. These findings parallel the periodic case. However, the variation in the adsorption energies with the sites of attachment as well as details of the adsorption geometries are, in many of the systems considered here, a direct manifestation of the confinement due to the finite size of the SWNTs considered here. For all hydrocarbon species examined, the favored places of adsorption are found in the tube termination zone where the strain of the SWNT substrate is highest. Comparison between the linear spin-density distributions for loaded and pure SWNTs allows to infer details about the impact of the SWNT magnetic structure on hydrocarbon adsorption and vice versa. Thus, maximum stability of CH bonding with the capped SWNT is found in the matching regime between the tube and the fullerene half where the finite SWNT is maximally strained. For truncated substrates, sites adjacent to terminating carbon decagon are determined to be the locations of preferential attachment for both CH and CH_2. The places of CH_3 adsorption and the site dependence of the CH_3 adsorption energies on the truncated SWNT mirror the sites and the sizes of linear spin density maxima along the SWNT. Attaching CH_3 to the capped SWNT results in a collapse of the SWNT magnetism in the SWNT half to which the molecule is attached.

The present project is to be continued in two directions. First, the conductivity of the finite nanotubes investigated here will be analyzed and in particular, the conductivity variation upon adsorption of hydrocarbon radicals will be recorded. Further, in order to explore the relevance of these systems for spintronics applications, we will focus on the influence exerted by the magnetic coordination of the SWNT on the electric resistance encountered by spin-polarized currents traversing the tube. Currently, we prepare this step by investigating the geometric, electronic, and magnetic properties of cross-linking SWNT architectures that consist of two SWNTs vertically connected by a third. Systems of this composition are of equal interest for nanomechanics and nanoelectronics. Their importance for the latter field of application is rooted in the realization that the two bounding SWNTs may serve as nanoelectrodes and the connecting SWNT as a nanoscopic transmission element. Adopting this

homogeneous arrangement for the study of SWNT conductivity eliminates the complex problem of matching the carbon nanotube ends to the surfaces of electrodes consisting of materials different from carbon. In a second step, the adsorption of molecular species of relevance for sensing applications will be addressed, involving chiefly explosives and biomolecules. This work was supported by the Department of Defense through the U.S. Army/Engineer Research and Development Center (Vicksburg, MS), Contract No. W912HZ-07-C-0073.

[1] X. Yang, R. Q. Zhang, and J. Ni, Phys. Rev. B **79**, 075431 (2009).
[2] P. Bondavalli, P. Legagneux, and D. Pribat, Sens. Actuators B Chem. **140**, 304 (2009); Y. Wang, Z. Zhou, Z. Yang, X. Chen, D. Xu, and Y. Zhang, Nanotechnology **20**, 345502 (2009); D. R. Kauffman and A. Star, Angew. Chem. Int. Ed. **47**, 6550 (2008); J. P. Novak, E. S. Snow, J. P. Hauser, D. Park, J. L. Stepnowski, and R. A. McGill, Appl. Phys. Lett. **83**, 4026 (2003); J. Kong, N. R. Franklin, C. Zhou, M. G. Chapline, S. Peng, K. Cho, and H. Dai, Science **287**, 622 (2000).
[3] L. Valentini, I. Armentano, D. Puglia, L. Lozzi, S. Santucci, and J. M. Kenny, Thin Solid Films **449**, 105 (2004).
[4] R. L. Zhou, H. Y. He, and B. C. Pan, Phys. Rev. B **75**, 113401 (2007).
[5] S. Hofmann, G. Csanyi, A. C. Ferrari, M. C. Payne, and J. Robertson, Phys. Rev. Lett. **95**, 036101 (2005).
[6] H. Y. He and B. C. Pan, Physica E **40**, 542 (2008).
[7] H. Y. He and B. C. Pan, J. Phys. Chem. C **112**, 18876 (2008).
[8] D. B. Hash, M. S. Bell, K. B. K. Teo, B. A. Cruden, W. I. Milne, and M. Meyyappan, Nanotechnology **16**, 925 (2005); B. A. Cruden, A. M. Cassell, D. B. Hash, and M. Meyyappan, J. Appl. Phys. **96**, 5284 (2004); M. Grujicic, G. Cao, and B. Gersten, Appl. Surf. Sci. **191**, 223 (2002)
[9] T. Yumura, S. Bandow, K. Yoshizawa, and S. Iijima, J. Phys. Chem. B **108**, 11426 (2004); T. Yumura, K. Hirahara, S. Bandow, K. Yoshizawa, and S. Iijima, Chem. Phys. Lett. **386**, 38 (2004); T. Yumura, D. Nozaki, S. Bandow, K. Yoshizawa, and S. Iijima, J. Am. Chem. Soc. **127**, 11769 (2005).
[10] Y. Higuchi, K. Kusakaba, N. Suzuki, S. Tsuneyuki, J. Yamauchi, K. Akagi, and Y. Yoshimoto, J. Phys.: Condens. Matter **16**, S5689 (2004).
[11] J. Wu and F. Hagelberg, Phys. Rev. B **79**, 115436 (2009).
[12] A. Mananes, F. Duque, A. Ayuela, M. J. Lopez, and J. A. Alonso, Phys. Rev. B **78**, 035432 (2008).
[13] A. J. Du, Y. Chen, G. Q. Lu, and S. C. Smith, Appl. Phys. Lett. **93**, 073101 (2008).
[14] B. Sitharaman, K. R. Kissell, K. B. Hartman, L. A. Tran, A. Baikalov, I. Rusakova, Y. Sun, H. A. Khant, S. J. Ludtke, W. Chiu, S. Laus, E. Toth, L. Helm, A. E. Merbach, and L. J. Wilson, Chem. Commun. **31**, 3915 (2005).
[15] E. H. Lieb, Phys. Rev. Lett. **62**, 1201 (1989).
[16] J. Hubbard, Proc. R. Soc. Lond. A **276**, 238 (1963).
[17] J. Fernandez-Rossier and J. J. Palacios, Phys. Rev. Lett. **99**, 177204 (2007).
[18] Y.-W. Son, M. L. Cohen, and S. G. Louie, Nature (London) **444**, 347 (2006).
[19] Y.-W. Son, M. L. Cohen, and S. G. Louie, Nature (London) **446**, 342 (2007); V. Barone, O. Hod, and G. E. Scuseria, Nano Lett. **6**, 2748 (2006).
[20] W. Kohn and L. J. Sham, Phys. Rev. **140**, A1133 (1965).
[21] G. Kresse and J. Hafner, Phys. Rev. B **47**, 558 (1993); **49**, 14251 (1994).
[22] G. Kresse and J. Furthmuller, Comput. Mater. Sci. **6**, 15 (1996).
[23] N. D. Mermin, Phys. Rev. **137**, A1141 (1965).
[24] J. P. Perdew and A. Zunger, Phys. Rev. B **23**, 5048 (1981).
[25] D. M. Wood and A. Zunger, J. Phys. A **18**, 1343 (1985).
[26] P. Pulay, Chem. Phys. Lett. **73**, 393 (1980).
[27] P. E. Blochl, Phys. Rev. B **50**, 17953 (1994).
[28] J. P. Perdew, K. Burke, and M. Ernzerhof, Phys. Rev. Lett. **77**, 3865 (1996).
[29] M. J. Frisch, G. W. Trucks, H. B. Schlegel, G. E. Scuseria, M. A. Robb, J. R. Cheeseman, J. A. Montgomery, Jr., T. Vreven, K. N. Kudin, J. C. Burant, J. M. Millam, S. S. Iyengar, J. Tomasi, V. Barone, B. Mennucci, M. Cossi, G. Scalmani, N. Rega, G. A. Petersson, H. Nakatsuji, M. Hada, M. Ehara, K. Toyota, R. Fukuda, J. Hasegawa, M. Ishida, T. Nakajima, Y. Honda, O. Kitao, H. Nakai, M. Klene, X. Li, J. E. Knox, H. P. Hratchian, J. B. Cross, V. Bakken, C. Adamo, J. Jaramillo, R. Gomperts, R. E. Stratmann, O. Yazyev, A. J. Austin, R. Cammi, C. Pomelli, J. W. Ochterski, P. Y. Ayala, K. Morokuma, G. A. Voth, P. Salvador, J. J. Dannenberg, V. G. Zakrzewski, S. Dapprich, A. D. Daniels, M. C. Strain, O. Farkas, D. K. Malick, A. D. Rabuck, K. Raghavachari, J. B. Foresman, J. V. Ortiz, Q. Cui, A. G. Baboul, S. Clifford, J. Cioslowski, B. B. Stefanov, G. Liu, A. Liashenko, P. Piskorz, I. Komaromi, R. L. Martin, D. J. Fox, T. Keith, M. A. Al-Laham, C. Y. Peng, A. Nanayakkara, M. Challacombe, P. M. W. Gill, B. Johnson, W. Chen, M. W. Wong, C. Gonzalez, and J. A. Pople, GAUSSIAN 03, Revision C.02, Gaussian, Inc., Wallingford CT, 2004.
[30] See supplementary material at http://link.aps.org/supplemental/10.1103/PhysRevB.81.155407 for C-C bond lengths related to CH and CH_2 adsorbates in contact with the truncated SWNT.